



## Effects of blending and coating methods on the performance of SIS (styrene-isoprene-styrene)-based pressure-sensitive adhesives

Dae-Jun Kim , Hyun-Joong Kim & Goan-Hee Yoon

To cite this article: Dae-Jun Kim , Hyun-Joong Kim & Goan-Hee Yoon (2004) Effects of blending and coating methods on the performance of SIS (styrene-isoprene-styrene)-based pressure-sensitive adhesives, Journal of Adhesion Science and Technology, 18:15-16, 1783-1797, DOI: [10.1163/1568561042708412](https://doi.org/10.1163/1568561042708412)

To link to this article: <https://doi.org/10.1163/1568561042708412>



Published online: 02 Apr 2012.



Submit your article to this journal [↗](#)



Article views: 70



Citing articles: 12 View citing articles [↗](#)

## Effects of blending and coating methods on the performance of SIS (styrene-isoprene-styrene)-based pressure-sensitive adhesives

DAE-JUN KIM<sup>1</sup>, HYUN-JOONG KIM<sup>1,\*</sup> and GOAN-HEE YOON<sup>2</sup>

<sup>1</sup> *Laboratory of Adhesion and Bio-Composites, Department of Forest Products,  
Seoul National University, Seoul 151-742, South Korea*

<sup>2</sup> *VIXXOL Corporation, Ansan 425-833, South Korea*

Received in final form 21 October 2004

**Abstract**—SIS (styrene-isoprene-styrene)-based pressure sensitive adhesives (PSAs) were prepared by melt- or solution-blending. In the coating process, two methods were used: solution coating and melt coating. The performances of the PSAs were found to be different, depending on which of these two blending or coating methods was used. In this study, we investigated the relationship between the viscoelastic properties and the performances of the SIS-based PSAs using different blending and coating methods. Three methods were used: (1) melt-blending and melt-coating, (2) melt-blending and solution-coating and (3) solution-blending and solution-coating. PSAs applied using melt-blending/melt-coating (M–M) have higher peel strength and probe tack than PSAs applied using melt-blending/solution-coating (M–S) and solution blending/solution coating (S–S). However, PSAs applied using M–M blends have lower holding power and SAFT (Shear adhesion failure temperature) than PSAs applied using M–S and S–S blends. The viscoelastic properties and GPC curves of M–S blends were similar to M–M blends, while the peel strength and tack of M–S blends were similar to S–S blends. Therefore, it was concluded that the blending process had more effect on the viscoelastic properties and shear creep of PSAs than the coating process.

**Keywords:** SIS (styrene-isoprene-styrene); tackifier; melt-blending/melt-coating; melt-blending/solution coating; solution-blending/solution coating; peel; tack; holding power; shear adhesion failure temperature (SAFT); viscoelastic properties.

### 1. INTRODUCTION

Styrenic block copolymer (SBC)-based PSAs can be prepared using either hot melt or solvent solution processes. Although solvent based SBC systems are still in use

---

\*To whom correspondence should be addressed. Tel.: (82-2) 880-4784. Fax: (82-2) 873-2318.  
E-mail: [hjokim@snu.ac.kr](mailto:hjokim@snu.ac.kr)

in some PSA tape and label applications, the trend is toward hot melt mixed and applied systems, so as to eliminate the need for solvents [1–3].

At room temperature, the polystyrene domain is stiff. By heating to temperatures above the glass transition temperature ( $T_g$ ) of the polystyrene, i.e., above 100°C, the domains begin to weaken [4–6]. Although the domains are softened at temperatures above 100°C, heating alone does not cause SBCs to melt and flow. They will not flow unless mechanical energy is also applied.

Generally, the SIS-based PSAs are prepared by melt- or solution-blending. The PSAs prepared by melt-blending are mixed in an internal mixer, such as a Brabender Plasticoder, at the melting temperature, while those prepared by solution-blending are mixed in a solvent, such as toluene, at ambient temperature. In the coating process, two methods are employed, i.e., solution coating and melt coating [7].

Nakajima *et al.* [8] investigated the rheological properties of SIS/tackifier-based PSAs applied using melt-blending/melt-coating. They reported that the  $T_g$  of melt-blended blends was about 10°C higher than that of solution-blended blends reported by Kraus and Hashimoto [9]. This is due to the difference in the preparation methods used to prepare the blends. Nakajima *et al.* [8] used melt-blending, while Kraus and Hashimoto [9] used solution-blending. There must be a significant difference in the resultant morphology in these two cases. However, the reasons for these differences have not been clearly elucidated.

In our previous study [10], we investigated the effect of blending methods on SIS-based PSAs. According to the results of that study, the performances and viscoelastic properties of the PSAs differed depending on the blending method used. However, the reasons for these differences were not clearly elucidated. O'Connor and Macosko [11] investigated the differences in hot-melt PSAs (HMPSAs) applied by melt coating and solvent coating. The HMPSAs were prepared using melt blending. They reported that the solvent-coated HMPSA showed better shear holding power, and the hot-melt-coated HMPSA performed better in tack and peel tests.

In this present study, we investigated the relationship between the viscoelastic properties and the performances of SIS-based PSAs using different blending and coating methods. Three methods were used (1) melt-blending and melt-coating, (2) melt-blending and solution-coating and (3) solution-blending and solution-coating.

## 2. EXPERIMENTAL

### 2.1. Materials

SIS (styrene-isoprene-styrene) materials selected for this study were diblock and triblock SIS. The diblock SIS was Kraton D-1107 (diblock content 15 wt% and styrene content 15 wt%, made by Kraton Polymer, Houston, TX, USA) and the triblock SIS was Vector 4111 (diblock content < 1 wt%, styrene content 18 wt%,

**Table 1.**

Characterization data of the polymers

Trade name	Type	Styrene content (wt%) <sup>a</sup>	Diblock content (wt%) <sup>a</sup>	$M_w^b$	$M_n^b$	$M_w/M_n^b$	$T_g^c$ (°C)	Manufacturer
Kraton D1107	Linear SIS	15	15	129 000	106 000	1.21	−61.0	Kraton Polymer
Vector 4111	Linear SIS	18	<1	114 000	108 000	1.06	−61.0	ExxonMobil

<sup>a</sup> Data supplied by the manufacturer.<sup>b</sup> Determined by GPC.<sup>c</sup> Determined by DSC.**Table 2.**

Properties of the tackifiers

Trade name	Type	Softening point (°C) <sup>a</sup>	$M_w^b$	$M_n^b$	$M_w/M_n^b$	$T_g^c$ (°C)	Manufacturer
Hikorez A-1100S	Aliphatic hydrocarbon	98	946	382	2.48	45.7	Kolon
Regalite R-125	Hydrogenated aromatic hydrocarbon	123	816	369	2.21	68.0	Eastman

<sup>a</sup> Determined by the Ring and Ball method. Data supplied by the manufacturer.<sup>b</sup> Determined by GPC.<sup>c</sup> Determined by DSC.

made by ExxonMobil). The characterization data of the polymers are given in Table 1.

The tackifiers selected for this study were Hikorez A-1100S (C-5, Kolon, Incheon, South Korea) and Regalite R-125 (Hydrogenated C-9, Eastman). The properties of the tackifiers are shown in Table 2.

## 2.2. Preparation of PSAs

**2.2.1. Melt-blending/melt-coating.** The PSA components were blended in an internal mixer at 170–180°C. An antioxidant, Irganox 1010, was used as a thermal stabilizer. The SIS/tackifier blend ratios were 30 : 70, 40 : 60, 50 : 50 and 60 : 40 by weight.

The PSA specimens were prepared by melt-coating onto a poly(ethylene terephthalate) (PET) film with an average thickness of 75  $\mu\text{m}$ , using an automatic film applicator with a hot-plate (Kee-Pae Trading, Seoul, South Korea) operated at 150°C. A bar coater No. 9 (wet thickness 20.6  $\mu\text{m}$ ) was used.

**2.2.2. Melt-blending/solution-coating.** The PSA components were blended in an internal mixer at 170–180°C. The SIS/tackifier blend ratios were 30:70, 40:60, 50:50 and 60:40 by weight. After melt-blending, the blends were dissolved in toluene at ambient temperature. Then, the PSA specimens were prepared by solution-coating onto a PET film with an average thickness of 75  $\mu\text{m}$ , using an automatic film applicator (Kee-Pae Trading) at room temperature. A bar coater No. 26 (wet thickness 59.4  $\mu\text{m}$ ) was used. The resulting PSA films were dried at 80°C for 10 min in an air circulation oven.

**2.2.3. Solution-blending/solution-coating.** The PSA components were blended in toluene at ambient temperature. The SIS/tackifier blend ratios were 30:70, 40:60, 50:50 and 60:40 by weight. The PSA specimens were prepared by solution-coating onto a PET film with an average thickness of 75  $\mu\text{m}$ , using an automatic film applicator (Kee-Pae Trading) at room temperature. A bar coater No. 26 (wet thickness 59.4  $\mu\text{m}$ ) was used. The resulting PSA films were dried at 80°C for 10 min in an air circulation oven.

### 2.3. Molecular weight

The weight average molecular weight ( $M_w$ ), the number average molecular weight ( $M_n$ ) and the molecular weight distribution ( $M_w/M_n$ ) of the PSAs (SIS/tackifier ratio 50:50) were determined by gel-permeation chromatography (GPC, Waters).

### 2.4. Thermal properties

The glass transition temperatures ( $T_g$ ) were measured using a differential scanning calorimeter (DSC, TA Instruments Q-1000, in NICEM at Seoul National University). The samples were first cooled to  $-80^\circ\text{C}$ , then heated to  $150^\circ\text{C}$  at a heating rate of  $5^\circ\text{C}/\text{min}$  (first scan). Then, they were immediately quenched to  $-80^\circ\text{C}$  and kept at this temperature for 5 min. The samples were then reheated to  $150^\circ\text{C}$  at a heating rate of  $5^\circ\text{C}/\text{min}$  (second scan). The  $T_g$  as defined in this study was obtained from the second scan to assure reproducible thermograms free from thermal history effects.

### 2.5. Viscoelastic properties

The viscoelastic properties (storage modulus, loss tangent and complex viscosity) of the blends were determined using ARES (Advanced Rheometrics Expansion System, Rheometric Scientific, at NICEM at Seoul National University) in the parallel plate (8 mm plate diameter) mode. A typical scan covered the range from  $-40^\circ\text{C}$  to  $120^\circ\text{C}$ .

### 2.6. Peel strength

The stainless steel substrate was cleaned with acetone. Then, the PSA specimen was pressed onto the stainless steel substrate using 2 passes with a 2-kg rubber roller.

The 180° peel strength of the PSA specimens coated onto PET was measured by tension at crosshead speeds of 75, 150, 300 and 600 mm/min at room temperature after keeping the specimens at these temperatures for 1 h.

### 2.7. Probe tack

The probe tack test was conducted using a texture analyzer (TA-XT2i, Micro Stable Systems, UK) with a polished stainless steel cylinder probe with a diameter of 5 mm. The measurements were carried out at separation rates of 0.1, 0.5, 1, 5 and 10 mm/s under a constant pressure of 100 g/cm<sup>2</sup> and a dwell time of 1 s.

### 2.8. Holding power ( $t_b$ , break time)

The holding power is characterized by the time (break time,  $t_b$ ) a PSA tape holds under a defined shear load [3]. The PSA specimen was pressed onto a stainless steel substrate (bonding area 25 mm × 25 mm) using 2 passes with a 2-kg rubber roller. The specimen was maintained at room temperature for 1 h. The holding power (break time,  $t_b$ ) was measured at 3 different temperatures (50, 70 and 90°C) and a load of 1 kg.

### 2.9. Shear adhesion failure temperature (SAFT)

Shear adhesion failure temperature (SAFT) gives information on the resistance of the PSA to stress at elevated temperature. The SAFT is the temperature at which the bond fails and the load drops [3]. The PSA specimen was pressed onto a stainless steel substrate (bonding area 25 mm × 25 mm) using 2 passes with a 2-kg rubber roller. The SAFT was measured at a heating rate of 0.4°C/min and a load of 1 kg.

## 3. RESULTS AND DISCUSSION

### 3.1. Molecular weight

The weight average molecular weight ( $M_w$ ) and the molecular weight distribution ( $M_w/M_n$ ) of the PSAs (SIS/tackifier ratio 50 : 50) were measured.

For all three blending and coating methods, neither  $M_w$  nor  $M_w/M_n$  exhibited significant differences. However, the shapes of the GPC curves showed some differences. The GPC curves of Vector 4111/Regalite R 125 blends are shown in Fig. 1.

The GPC curve of the melt-melt blend was similar to that of the melt-solution blend, while the GPC curve of the solution-solution blend had a different shape. The curve width of the melt-blended/melt-coated (M—M) blend was broader than that for the solution blended/solution coated (S—S) blend. Also, two peaks were observed in the case of the M—M blend and the melt-blended/solution coated (M—S) blend. This is perhaps due to thermal decomposition depending on the

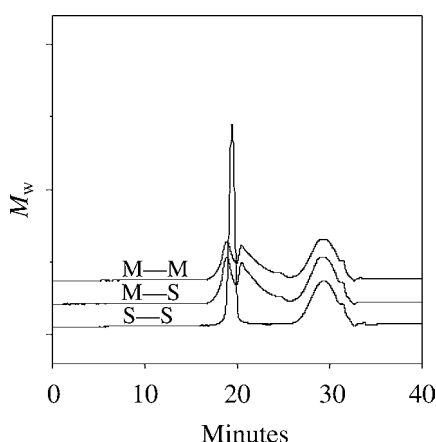


**Figure 1.** GPC curves of Vector 4111/Regalite R-125 (50 : 50) blends.

environmental conditions (time, temperature, oxygen, etc.). Therefore, there may be some differences in the resulting morphology, which would account for the differences in performance.

Generally, a very important aspect in melt processing of SBCs is the control of blending environment and other process parameters such as the temperature, time, mechanical shear and the presence of oxygen. Thermal decomposition must be avoided, as noted above. Additionally, oxidative degradation must be minimized when processing unsaturated midblock SBCs. Degradation in styrene-butadiene-styrene (SBS) leads to an increase in viscosity, gel formation and loss of tack, while in SIS it leads to lower viscosity, reduced cohesive strength and lower elevated temperature performance [2, 5].

Therefore, it is expected that the performance of melt-blended blends would differ from that of solution-blended blends, especially in terms of their cohesive strength.

### 3.2. Thermal properties

DSC has become a classical method for the determination of miscibility. The phase structure of each blend was assessed by measuring the number of glass transitions observed in the thermograms, as well as their temperatures. Two transitions are a clear indication of phase separation, while a single glass transition located at a temperature in between the glass transition temperatures of the pure components indicates miscibility [6, 12].

According to Refs. [13, 14], miscible blends have composition-dependent  $T_g$  values.

The  $T_g$  values of Vector 4111/Hikorez A-1100S blends are shown in Fig. 2. In all blends, only one well-defined glass transition lying between the glass transitions of the pure components is detected and it changes gradually according to the composition. The existence of a single composition-dependent  $T_g$  is evidence that the SIS materials used in this study (Kraton D-1107 and Vector 4111) are miscible

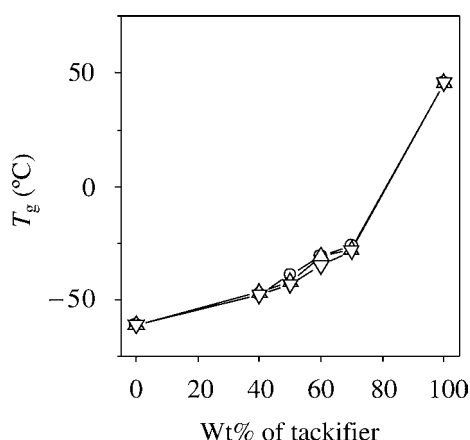


**Figure 2.** The  $T_g$  of Vector 4111/Hikorez A-1100S blends. (○) Melt-melt, (△) melt-solution, (▽) solution-solution.

with the tackifiers used in this study (Hikorez A-1100 S, Regalite R-125) below the  $T_g$ .

However, for all three methods of blending and coating there was no significant difference in  $T_g$ . This may be due to the characteristics of the DSC analysis method. It is expected that the resolving ability of DSC is too low for analyzing differences in different blending/coating methods. Therefore, the measurement of  $T_g$  by dynamic mechanical measurements (ARES, Advanced Rheometrics Expansion System, or DMTA, Dynamic Mechanical Thermal Analysis) is needed.

In our previous study [10], we measured the  $T_g$  of M–M blends and S–S blends by ARES. According to the results of this study, the  $T_g$  of the M–M blends was about 3–7°C higher than that of the S–S blends.

Also, Nakajima *et al.* [8] reported that the  $T_g$  (using Rheometrics Mechanical Spectrometer) of the melt-blended blends was about 10°C higher than that of the solution-blended blends reported by Kraus and Hashimoto [9]. However, the reasons for these differences were not clearly elucidated.

### 3.3. Viscoelastic properties

The viscoelastic properties of Kraton D-1107/Hikorez A-1100 S (40/60) blends are shown in Figs 3 and 4. As shown in these figures, the  $G'$  (storage modulus) and viscosity of the S–S blends were higher than those of the other blends, while the  $\tan \delta$  of the S–S blends was lower than those of the other blends. The order of  $G'$  and viscosity were S–S  $\gg$  M–S  $\approx$  M–M blends, while the order of  $\tan \delta$  was M–M  $\approx$  M–S  $\gg$  S–S. This may be due to thermal decomposition during melt-blending.

As indicated in the section on results of the GPC measurements, the curve width of the M–M blends was broader than that of the S–S blends. Also, two peaks were observed in both M–M and M–S blends. This may be due to thermal



decomposition during melt blending. Thus, there may be some difference in the resulting morphology, which would account for the differences in the viscoelastic properties. Therefore, it is thought that the blending process had more effect on the viscoelastic properties of the PSAs than the coating process.

Nakajima *et al.* [8] reported that the crossover temperature (where storage modulus,  $G'$  = loss modulus ( $G''$ ) at the higher temperature end of the rubbery plateau) was related to the shear creep resistance.

The crossover temperatures of Kraton D-1107/Hikorez A-1100S blends, prepared by the three methods (M–M, M–S, S–S), were 83.7°C, 85.5°C and 94.4°C, respectively. The crossover temperatures for the Kraton D-1107/Regalite R-125 blends, prepared by the three methods (M–M, M–S, S–S), were 81.8°C, 88.2°C

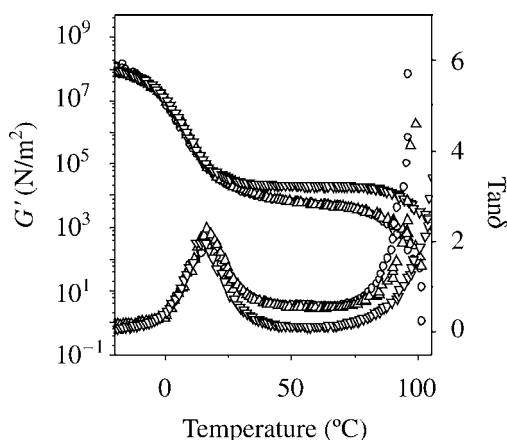


**Figure 3.** Viscoelastic properties of Kraton D-1107/Hikorez A-1100S (40 : 60) blends. (○) Melt-melt, (△) melt-solution, (▽) solution-solution.

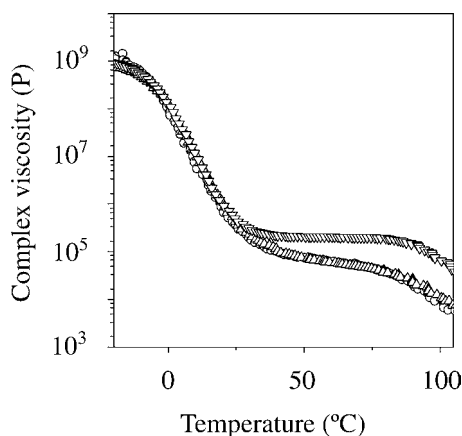


**Figure 4.** Complex viscosity of Kraton D-1107/Hikorez A-1100S (40 : 60) blends. (○) Melt-melt, (△) melt-solution, (▽) solution-solution.

and 95.2°C, respectively. The order of the crossover temperature was S—S  $\gg$  M—S > M—M blends.

Therefore, it is thought that the crossover temperature was related more to the blending process than to the coating process.

### 3.4. Peel strength

The 180° peel strength of the Kraton D-1107/Hikorez A-1100 S (40/60) blends at various peel rates is shown in Fig. 5.

As shown in Fig. 5, the peel strength of M—M blends was higher than those of the other blends. The order of the peel strength was M—M  $\gg$  M—S  $\approx$  S—S blends. This may be due to the cohesive failure mode. Cohesive failure or stick-slip occurred in the M—M and M—S blend samples, while interfacial failure occurred in the S—S blend samples.

Also, the M—M blends were exposed to higher temperatures. These processes were attributed to polymer chain scission and thermal degradation. There may be some differences in the resulting morphology, which would account for the differences in performance.

As the extent of lower molecular weight segment was increased, the cohesive strength and heat resistance decreased, while tack increased. These phenomena may be attributed to the lower peel strength of the S—S blends, as well as to the lower initial tack.

As indicated in the section on the results of GPC measurements, the shapes of the GPC curves showed some differences. This may be due to different extents of thermal decomposition depending on the environmental conditions (time, temperature, oxygen, etc.). Therefore, there may be some differences in the resulting morphology, which would account for the differences in performance.

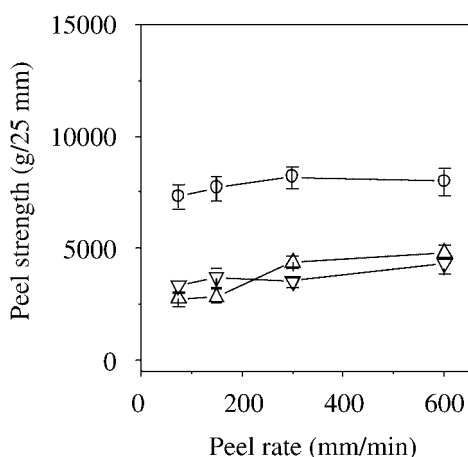


**Figure 5.** 180° peel strength of Kraton D-1107/Hikorez A-1100S (40:60) blends as a function of peel rate. (○) Melt-melt, (△) melt-solution, (▽) solution-solution.

When degradation occurs in the SIS, the result is lower viscosity, reduced cohesive strength and lower elevated temperature performance [1, 2, 5].

However, the phase separation of the S–S blends may be responsible for their inferior performance. Therefore, the peel strength of the S–S blends was lower than that of the M–M blends.

In our previous study [10], we investigated the peel strength of M–M blends and S–S blends. According to the results of that study, the peel strength of M–M blends was higher than that of the S–S blends. The results of that previous study [10] were similar to those obtained in the present study. O'Connor and Macosko reported that a hot-melt-coated HMPSA performed better than a solution-coated HMPSA in peel tests [11].

In terms of the type of tackifier used, the peel strength of Hikorez A 1100S blends was higher than that of Regalite R 125 blends. This is due to differences in the tackifier properties and tackifier content at maximum peel strength. Thus, to examine the effect of the tackifier, the results of the peel test at various tackifier contents were plotted in Fig. 6.

The blend made using Hikorez A-1100S has a maximum peel strength at 60 wt% of tackifier content, while the blend made using Regalite R-125 has a maximum peel strength at 40–50 wt% tackifier content. Similar results were obtained for all three blending and coating methods.

Regalite R 125 has a high softening point as well as  $T_g$ , and the PSAs made with this tackifier are brittle. Thus, the position of maximum peel strength with Regalite R-125 shifts to a lower tackifier content.

In our previous study [10], the position of maximum peel strength obtained with Regalite R-125 shifted to higher tackifier content in both M–M and S–S blends.

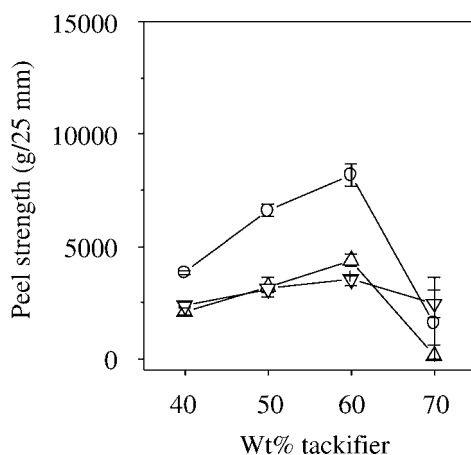


**Figure 6.** 180° peel strength of Kraton D-1107/Hikorez A-1100S blends as a function of tackifier content (peel rate 300 mm/min). (○) Melt-melt, (△) melt-solution, (▽) solution-solution.

### 3.5. Probe tack

The probe tack values for Vector 4111/Hikorez A 1100 S (40/60) blends at various separation rates are shown in Fig. 7.

As shown in Fig. 7, the probe tack of the M–M blend was higher than those of the other blends. The order of the probe tack was M–M  $\gg$  M–S  $>$  S–S blends. These results were similar to those obtained for the peel strength.

As the test mode used to determine the probe tack was similar to that used to measure the peel strength (mode I), it was expected that the results obtained for the probe tack would be similar to those obtained for the peel strength. As indicated in the section on the peel strength results, thermal decomposition can be attributed to higher tack. Therefore, the M–M blends, which were exposed to higher temperatures during blending and coating, have higher tack and lower cohesive strength.

In terms of the type of tackifier used, similar results were obtained. The probe tack of the Hikorez A-1100S blends was higher than that of the Regalite R-125 blends. This is due to differences in tackifier content at maximum probe tack. The results obtained for the probe tack at various tackifier contents are plotted in Fig. 8.

The blends made using Hikorez A-1100S have a maximum probe tack at 50–60 wt% of tackifier content, while the blends made using Regalite R-125 have a maximum probe tack at 40 wt% tackifier content. Similar results were obtained for all three blending and coating methods.

Regalite R-125 has a higher softening point, as well as a higher  $T_g$ , than Hikorez A-1100S and PSAs with this tackifier are brittle. Thus, the position of the maximum probe tack with Regalite R-125 shifts to lower tackifier content. The results obtained for the probe tack were similar to those obtained for the peel strength.

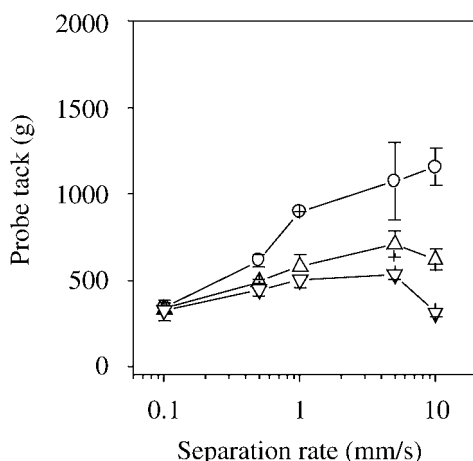


**Figure 7.** Probe tack of Vector 4111/Hikorez A-1100S (40:60) blends as a function of separation rate. (○) Melt-melt, (Δ) melt-solution, (▽) solution-solution.

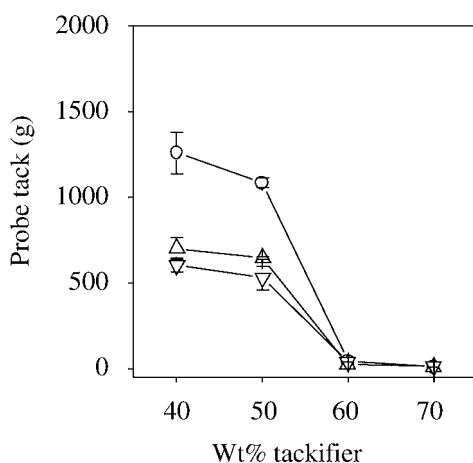


**Figure 8.** Probe tack of Kraton D-1107 / Regalite R-125 blends as a function of tackifier content (separation rate 10 mm/s). (○) Melt-melt, (△) melt-solution, (▽) solution-solution.

In terms of the SIS type, the Vector 4111/tackifiers blends exhibit maximum tack values at higher tackifier contents than the Kraton D 1107/tackifier blends. This is due to the fact that the triblock SIS (Vector 4111) has a higher cohesion than the diblock SIS (Kraton D-1107).

### 3.6. Holding power and shear adhesion failure temperature

The holding power and shear adhesion failure temperature (SAFT) of Kraton D-1107/Hikorez A-1100S blends as a function of tackifier content are shown in Figs 9 and 10, respectively.

As shown in Fig. 9, the holding power of the S–S blends was higher than those of the other blends. The order of holding power was S–S  $\gg$  M–S > M–M blends. These results show an opposite trend compared to the peel strength and probe tack. In terms of the SAFT (Fig. 10), similar results were observed. This is due to thermal degradation of the polymer during melting. As shown in Fig. 1 (GPC curves), the GPC curve of the M–M blend was similar to that of the M–S blend, while the GPC curve of the S–S blend had a different shape. As indicated in the section on the GPC results, the broader curve observed in the case of the M–M and M–S blends was related to thermal decomposition. O'Connor and Macosko reported that a solvent-coated PSA showed higher holding power [11].

Cohesion increases with increasing molecular weight. The influence of the molecular weight on the shear resistance is illustrated by the changes in shear resistance due to adhesive aging (i.e., degradation and depolymerization). SIS block copolymers undergo oxidative degradation at elevated temperatures by a mechanism which leads predominantly to scission of the polymer chains. This leads to a drop in molecular weight and thus to a decrease in both viscosity and holding power [6].

The composition of the adhesive (i.e., its nature and molecular weight) influences the shear. The dependence of the shear on the molecular weight is illustrated

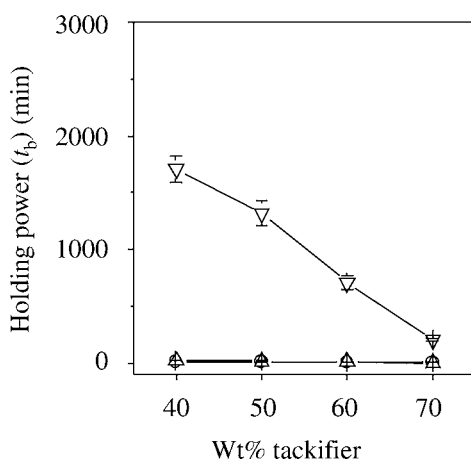


**Figure 9.** Holding power at 70°C of Kraton D-1107/Hikorez A-1100S blends as a function of tackifier content. (○) Melt-melt, (△) melt-solution, (▽) solution-solution.

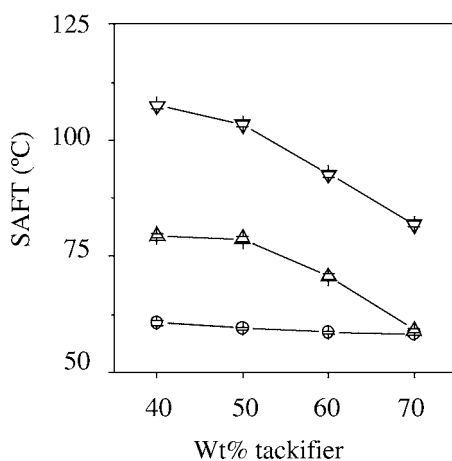


**Figure 10.** Shear adhesion failure temperature (SAFT) of Kraton D-1107/Hikorez A-1100S blends as a function of tackifier content. (○) Melt-melt, (△) melt-solution, (▽) solution-solution.

by melt-blending of HMPSAs. Dramatic reductions in both melt viscosity and holding power result from even a partial degradation. The shear depends on the molecular weight and its distribution (MWD). A polymer with a broad MWD has a lower cohesive strength than the one with a narrow MWD and a low molecular weight. The shear resistance is improved by an increase in the melting point of the resin [1, 2, 6].

As indicated above, the broader GPC curves for the M–M and M–S blends were related to their broad MWD, and therefore the M–M and M–S blends have lower cohesive strengths than blends which have a narrow MWD (sharp curve).

The S–S blends were not affected by the heat during blending and coating, but M–S blends were affected by the heat during coating. However, the M–M blends

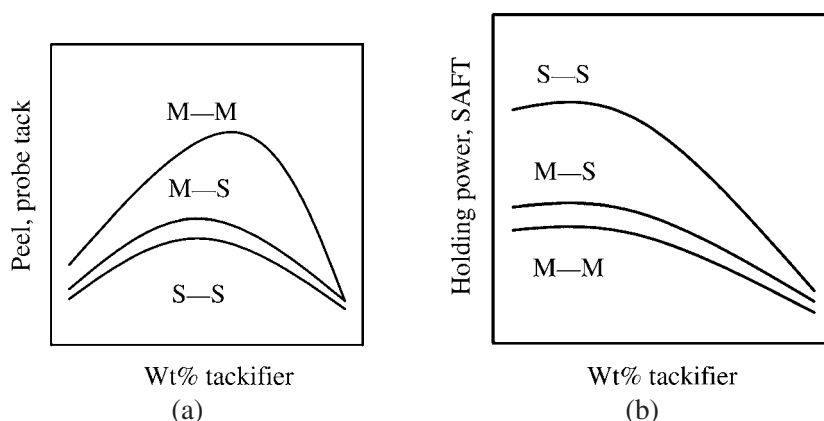


**Figure 11.** A schematic illustration of the effects of blending and coating methods on performance of SIS-based PSAs. (a) Peel strength and probe tack, (b) holding power and SAFT.

were affected by the heat during both blending and coating. Although Regalite R-125 and Vector 4111 are high thermal resistance materials, similar results were observed in the blends made using these two materials.

### 3.7. Schematic illustration

A schematic illustration of the effects of blending and coating methods on the performance of SIS-based PSAs is shown in Fig. 11. As shown in Fig. 11, PSAs applied using melt-blending/melt-coating (M–M) have higher peel strength and probe tack than PSAs applied using melt-blending/solution-coating (M–S) and solution blending/solution coating (S–S). But, PSAs applied using M–M blends have lower holding power and SAFT than PSAs applied using M–S and S–S blends.

This is due to difference in morphology and formation of lower-molecular-weight segments during thermal processing (melt blending or melt coating).

## 4. CONCLUSIONS

Pressure-sensitive adhesives (PSAs) applied using M–M blends have higher peel strength and probe tack than PSAs using M–S and S–S blends. But, PSAs applied using M–M blends have lower holding power and SAFT than PSAs applied using M–S and S–S blends.

The melting processes were attributed to polymer chain scission and thermal degradation. In the GPC results, the curve width of the M–M blends was broader than that of the S–S blends. There may be some differences in the resulting morphology, which would account for the differences in performance. The broader GPC curves for the M–M and M–S blends were due to their broad MWD and, therefore, the M–M and M–S blends have a lower cohesive strength than blends with a narrow MWD (sharp curve).

Also, the viscoelastic properties of M–S blends were similar to M–M blends, while peel and tack of M–S blends were similar to S–S blends. Therefore, it is thought that the mixing process had more effect on the viscoelastic properties and shear creep of PSAs than the coating process.

Because the test mode used for measuring the probe tack was similar to that used for measuring the peel strength (mode I), it was expected that similar results would be observed in both cases. However, the holding power, which was measured in mode II, gave different results.

### Acknowledgements

This work was partially supported by Brain Korea 21 Project and Vixxol Corporation.

### REFERENCES

1. I. Benedek and L. J. Heymans, *Pressure Sensitive Adhesives Technology*. Marcel Dekker, New York, NY (1996).
2. F. C. Jagisch and J. M. Tancrede, in: *Handbook of Pressure Sensitive Adhesives*, D. Satas (Ed.), pp. 346–398. Satas & Associates, Warwick, RI (1999).
3. G. Gierenz and W. Karmann, *Adhesives and Adhesive Tapes*. Wiley-VCH, Weinheim (2001).
4. M. Dupont and N. De. Keyzer, in: *Proceeding of Pressure Sensitive Tape Council 17th Annual Technical Seminar*, Schaumburg, IL (1994).
5. D. R. Hansen, E. E. Ewins and D. J. St. Clair, *Kraton™ Polymer — Formulating Guide for Adhesives and Sealants*. Kraton Polymer, Houston, TX (2000).
6. A. V. Pocius, *Adhesion and Adhesives Technology*, 2nd edn. Hanser, Munich (2002).
7. I. Benedek, *Development and Manufacture of Pressure-Sensitive Products*. Marcel Dekker, New York, NY (1999).
8. N. Nakajima, R. Babrowicz and E. R. Harrell, *J. Appl. Polym. Sci.* **44**, 1437–1456 (1992).
9. G. Kraus and T. Hashimoto, *J. Appl. Polym. Sci.* **27**, 1745–1757 (1982).
10. D.-J. Kim, Y.-J. Park and H.-J. Kim, in: *Proceedings of the 40th Annual Meeting of the Adhesion Society of Japan*, Tokyo (2002).
11. A. O'Connor and C. Macosko, *J. Appl. Polym. Sci.* **86**, 3355–3367 (2002).
12. S. Hayashi, H.-J. Kim, M. Kajiyama, H. Ono, H. Mizumachi and Z. Zufu, *J. Appl. Polym. Sci.* **71**, 651–663 (1999).
13. H.-J. Kim and H. Mizumachi, *J. Appl. Polym. Sci.* **56**, 201–209 (1995).
14. M. Fujita, M. Kajiyama, A. Takemura, H. Ono, H. Mizumachi and S. Hayashi, *J. Appl. Polym. Sci.* **64**, 2191–2197 (1997).